OPERATION AN]) PERFORMANCE OF A SECOND GENERATION, Sol,11) STATIC, STAR TRACKER, THE ASC

Allan Eisenman
Jet Propulsion 1 aboratory, California Institute of Technology
Pasadena, CA 91109 -8O99

Carl Christian 1 iebe
1 Department of Automation, The Technical University of 1 Denmark
2800 Lyngby, Denmark

ABSTRACT

The Advanced Stellar Compass (ASC) is a second generation star tracker, consisting, of a CCI) carom and its associated microcomputer. The ASC operates by matching the star images acquired by the camera with its internal star catalogs. An initial attitude acquisition (solving the lost in space problem) is performed, and successively, the attitude of the camera is calculated in celestial coordinates by averaging the position of a large number of star observations for each image. Key parameters of the ASC for the Ørsted satellite and Astrid II satellite versions am: mass as low as 900" g, power consumption as low as 5.5W, relative attitude angle errors less than 1.4 arcseconds in declination, and 13 arcseconds in roll, RMS, as measured at the Mauna Kea, 111 observatories of the University of 1 Iawaii in June 1996.

1.1 N']']< ()])UCTION

1 Denmark recentl y completed building its fi rst satel lite, Ørsted[1], A preci sion star tracker is an integral part of its science payload. During the initial design phase of Ørsted in 1993, the availability of a low-mass, low-power, low-residual-magnetism star tracker with high accuracy and autonomy was investigated. The study disclosed that it was not possible to acquire a commercial star tracker with the required specifications. Subsequently, the Technical University of Denmark was selected to design and build the Advanced Stellar Compass (ASC), a second generation, so]icl-state, stat tracker, for Ørsted.

The first follow-on mission that will use the ASC after Orsted, is the Swedish ASTRID II satellite [2] which is spin stabilized at x" per s. Also, the ASC has been accepted as the baseline stellar reference unit for the Pluto Express mission, During this investigation, the accuracy of the ASC was evaluated at the Mauna Kea, 111 observatories, of the 1 Jniversity of Hawaii in June 1 ')96.

2. '1'1 IE ADVANCED STELLAR COMPASS

Typically, a conventional star tracker consists of a CCI)-based star camera and its integral image processing electronics. '1 he elect ronics process the images for a number of bright stars (?-6) and outputs their centroids in CCI) coordinates. '1 he main computer onboard the spacecraft then identifies the stars and transforms the tracker output into celestial coordinates [3][4][5] as represented in Fig. 1.

Second generation, solid-stale, star trackers, such as the ASC and the AST [6], also centroid the images. However, the star identification and image coordinate transformation are performed autonomously using internal star catalogs. '1 he ASC consists of separate camera and electronics units. The entire star image frame is transferred from the camera to the microprocessor which

processes the whole frame. First, the ASC compares the stars of one full image frame to the whole acquisition catalog to identify the stars in the FOV and to make a course determination of the pointing, direction of the camera in celestial coordinates. Then, a precision comparison is done to the larger tracking catalog on each subsequent image frame as long as tracking is maintained, and the full accuracy pointing direction is determined.

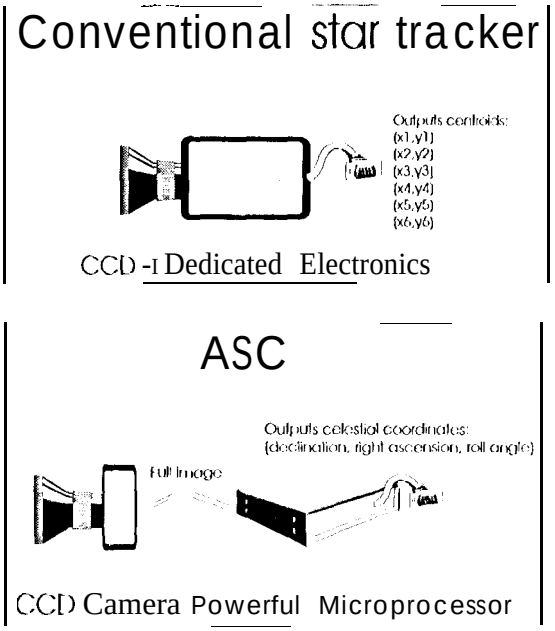

Figure 1. Representations of conventional star tracker and ASC.

The ASC star camera (Fig. 2) is based on a commercial Sony camcorder CCD chip, CDX039AL. The lens is custom designed for the camera. It has a focal length of 16 mm and focal ratio of f/0.7. Its point-spread function is designed to cover an area on the CCD chip of about 6 pixels in diameter. This is accomplished with a minimum of defocussing and optimizes the precision of star image centroid extraction [7].

The flight computer is a SO-MI Iz 80486 type of processor, using 4 Mbytes of RAM, 2 Mbytes of flash memory, multiple protection mechanisms, and fuselinked boot strap. Precision timing which enables astronomical corrections is obtained from a Global Positioning System receiver [8].

The ASC operation is initiated by acquiring a star image. Since no a priori knowledge of the orientation exists, the microprocessor performs a pattern recognition of the image as per the published algorithms [9][10]. The complexity of the problem is illustrated in Fig. 3 which shows how a (Xl]) image containing, 12 stars is matched to a star catalog containing the 2200 brightest stars. This process takes less than 1 second!

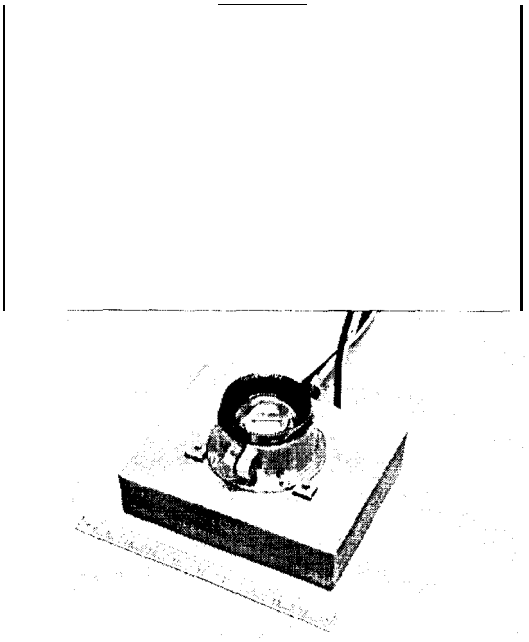

Figure 2. Flight and engineering models of the Ørsted star camera.

Since the attitude acquisition process determines an approximate attitude, it is then possible to refine the attitude by first generating a reference star pattern based on the tracking star catalog. The reference pattern covers the star camera field of view. The real star and the artificial stat patterns should be very similar. A spherical least squares fit is performed between them [11]. The

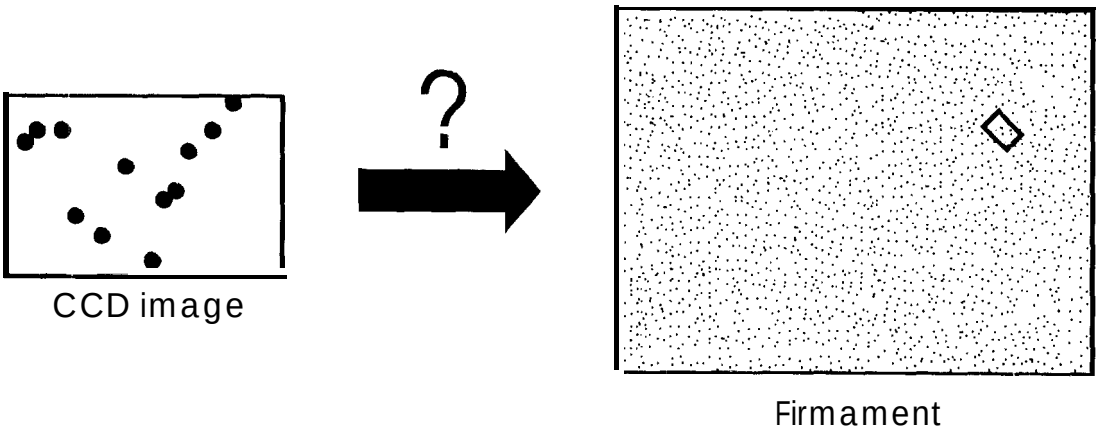

Figure 3. Illustration of the initial attitude acquisition, matching the CCD image to the firmament.

Table 1. Key parameters of ASC variants

PARAMETERS	Ø(m)	AII(p)	1 (m)	111'(]))
Star sensitivity threshold, M_1	6.()	5,5	6.0	9.5
Noise equivalent angle, 1 axis, Rh4S	0.9	1 . 5	--1.0	0.30
Acquisition data base, number of stars	2,000	1,836	1,836	42,654
Tracking data base, number of stars	10,'731	9,375	9,375	231,435
Relative accuracy, 1 axis, RMS error, arcsec	1.4	5	2.0	0.63
Mass, camera head, Kg	0.13	0.20	0.95	1 .?
Mass, processing electronics, Kg	1.4	0.80	0.90	1.0
Power consumption, camera head, W	().s	0.4	0.4	0.4-
Power consumption, proc. elec's, W	5.()	7.0	6.()	1"1.0
Field of view, degrees	1 6x22	1 6x22	16x22	"3.3X4.5
Update rate, Hz	1	2	2	1
Permissible radiation dosage, KRad	]0	10	100	100

Ø: Ørsted, AI I: ASTRID 11, HP: 1 high Precision, I: Interplanetary
m: measured, p: projected

resulting attitude estimate is then corrected for various astronomical effects (aberration, precession, nutation) [12] in order to obtain the output quarternion.

Some key physical parameters of different versions of the. ASC are shown in Table 1.

3. THE ME ASUREMENTS AT MAUNA KEA

In June 1996, the ASC was taken to the observatories of the University of' 1 lawaii on Mauna Kea, III. The purpose Of this trip was to determine the accuracy of the ASC with a minimal perturbing airmass. Two University of 1 lawaii telescopes were used for observation, as shown in Fig. 4.

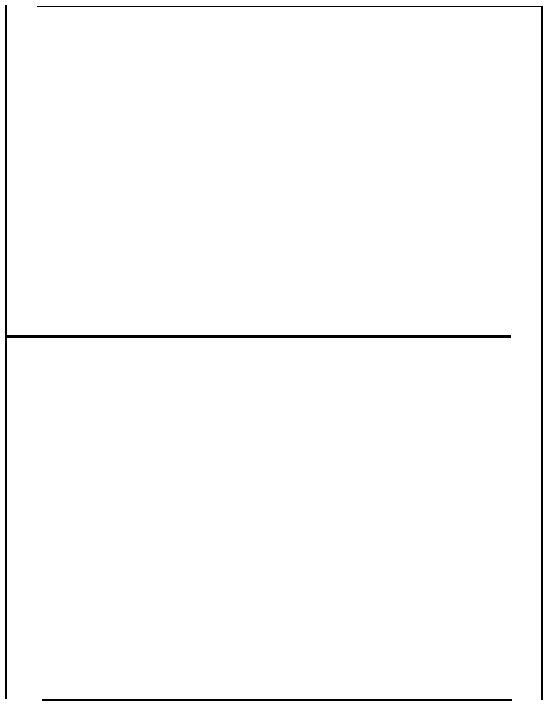

Figure 4. University of 1 lawaii 24" and 88" telescopes with ASC CHU.

Two kinds of' accuracy were determined: the noise equivalent angle (NEA) and the relative accuracy [13]. The NEA is defined as the variation in the calculated attitude of the ASC when it views a constantly positioned star field, It includes both source and system noise terms, i .c., photon noise, dark current noise, etc. the NEA is measured utilizing a telescope as an ASC mount and tracking a specific part of the sky. It should be noted that the measurements include non-ASC artifacts such as at mospheric pert urbat ions and telescope pointing jitter. The data gathered at Mauna Kca included 727 images. Atmospheric refraction is not corrected for in the measurements. The measured angles arc shown in Fig. 5.

Relative accuracy was the other parameter which was evaluated. It is defined here, as the NJ EA plus the systematic errors including non-optima] lens correcting function, error in the subpixel position interpolation function, errors caused by the effect of stars leaving and entering the camera FOV, etc.. The error in relative accuracy is measured by pointing the star camera toward the sky zenith anti acquiring continuous attitude data while stars drift through the camera FOV at the sidereal rate. Assuming that the epoch and equinox of the star catalog, are the same as the observing time, the declination and roll angles remain constant, whereas the right ascension increases with the sidereal rate. The data acquired at Mauna Kea included a zenith pointing, series in excess of 2 hours and including 2578 images. The attitude angles are shown in Fig. 6. Right ascension is not shown, because it is dominated by the sidereal rate.

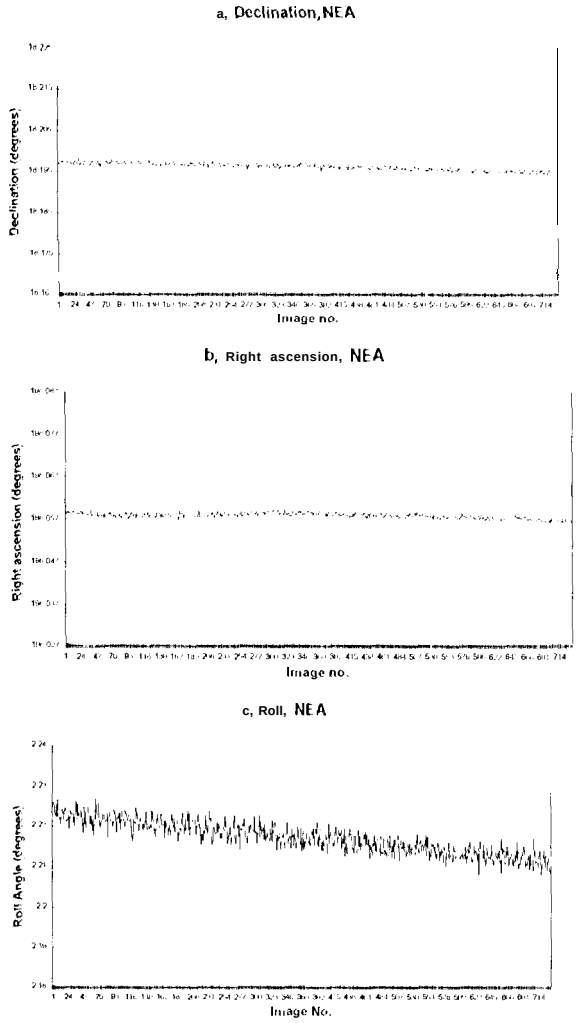

Figure 5. Tracking series attitude angle measurements..

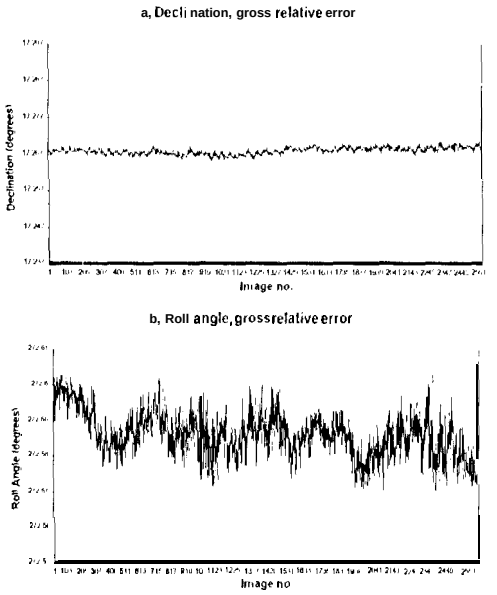

Figure 6. Zenith series attitude angle measurements.

4. RELATIVE ACCURACY MEASUREMENTS

Relative accuracy is a dynamic characterization of the ASC because it based on changing star fields. While relative accuracy includes the previous ident i fied error terms, it should be noted that the data has been acquired over a period of hours. This means that artifacts such as air stability, thermal displacement of the camera, changing moon light, telescope drift arc also included in the attitude angles. These phenomena are not directly related to the instrument performance and should be subtracted in order to determine the true instrument performance. Generally, these effects vary slow] y with time and can be removed from the signal by taking the Fourier transform of the original time domain signal, subtracting low frequencies which are dominated by the slowly varying artifacts and then applying an inverse transformation back to the time domain. The resulting signal is a more accurate representation of the inherent errors in the instrument with suppression of the terrestrial artifacts. '1 he effect of subtracting frequency below 0.0051 Iz is shown in Fig. 7. The signal component corresponding to the slowly varying artifacts arc shown in a. and rapidly varying signal primarily corresponding to i nstrument errors is shown in b.

It is difficult to define a specific frequency between external artifacts and internal instrument errors, because the artifacts arc not quantified. in Fig. 8, the x axis's represents the lowest frequencies not removed from the unprocessed data and the y axis's the RMS noise (in arcseconds). As an example, if the relative accuracy (zenith pointing) of the roll angle is defined as all frequencies higher than 0.1 1 Iz, then its value is 9 arcseconds RM S.

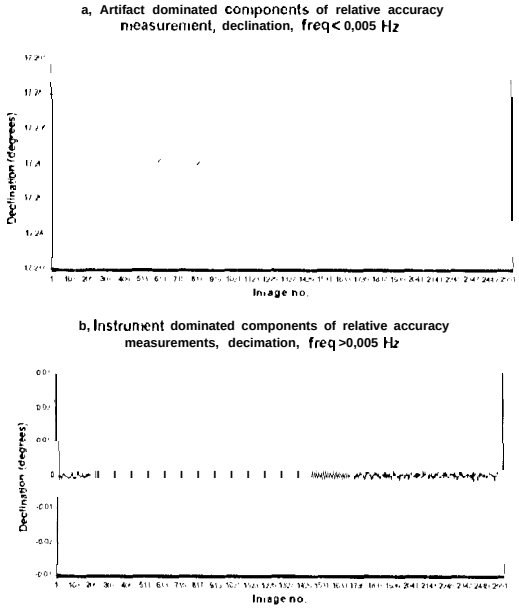

Figure 7. Slow and fast varying components of declination angles from the zenith pointing series.

Judging by the shape of the spectral noise in Fig. 8, it appears that tbc dominant middle part of the curve is white noise, as the RMS decreases constantly with the frequencies. Also (as expected) there arc no remaining frequencies at O.15 117,, which is half of the sampling frequency. '1 he peak at the low frequency part is believed to be mostly due to external terrestrial artifacts. Based on this conservative

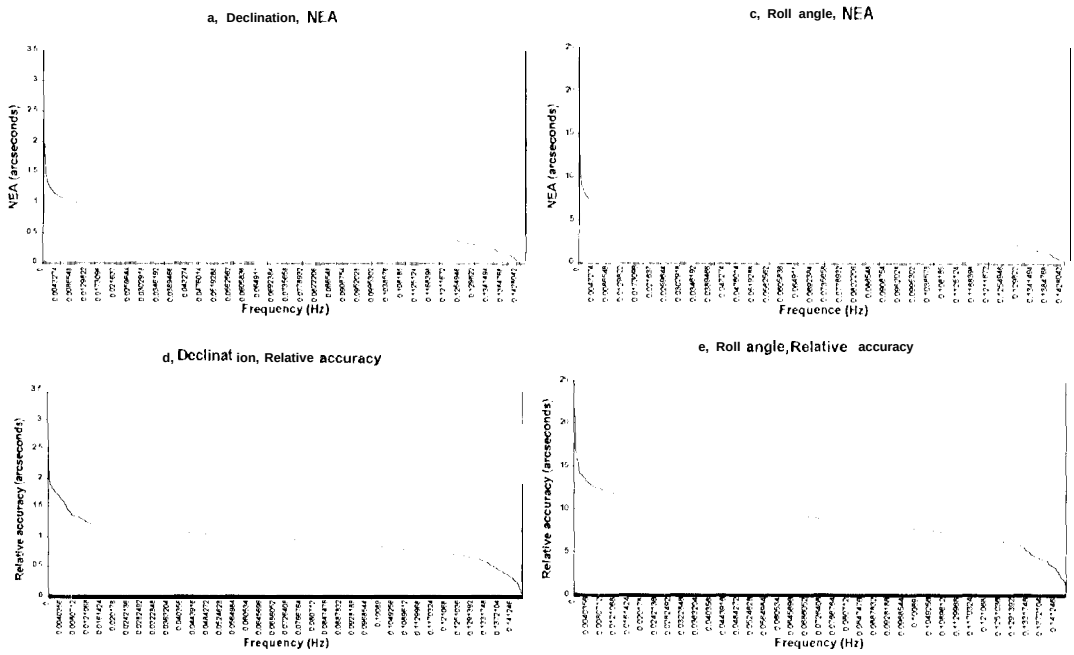

Figure 8. RMS NEA and relative accuracy vs. bandwidth.

Table 2. ASC Performance Summary

	Declination	Right ascension	Roll angle
NEA (RMS)	1.1"	1.2"	8' 8"
Relative accuracy (RMS)	1.4"	NA	1' 13"

estimate of terrestial artifacts, NEA and relative accuracy are given in Table 2.

5. SYSTEMATIC ERRORS

A very powerful tool to evaluate systematic errors in the ASC is to draw an error vector diagram. The error vector diagram is a representation of the CCD image. For each observed star a vector is drawn toward the corresponding star in the star catalog and the length of the vector is proportional to the distance. An error vector diagram of an image from the zenith pointing series is shown in Fig. 9.

The average length of the error vectors is 15 arcseconds. The error vector diagram can be used to disclose if all error vectors are randomly orientated. For example, if all error vectors point toward the center of the image, the value of the focal length of the lens will be adjusted to eliminate the effect and only leave the random terms.

A single error vector diagram, however, does not indicate much about systematic errors. Therefore, it is of interest to display successive error vector diagrams imposed on the same frame. This is depicted in Fig. 10.

The error vector diagram covers a sequence of 200 images from the Zenith series. This can be used to identify statistical fluctuations (NEA) and systematic errors. Where the error vectors for a star point in the same direction, it is indicative of an error in the star database.

Also, it can be seen in Fig. 10 that the errors in the X direction are greater than those in the Y direction. This is as yet unexplained, but may be indicative of systematic errors which can be reduced

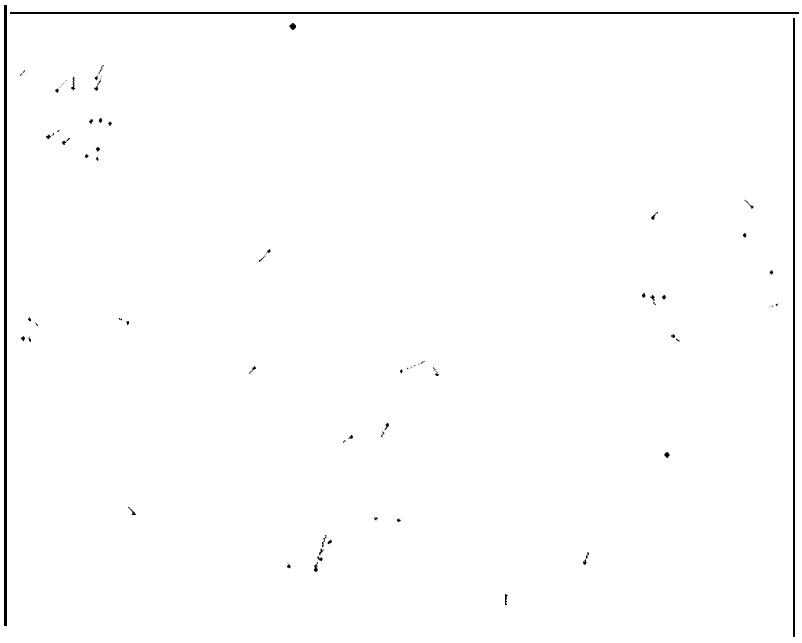

Figure 9. An error vector diagram from a single frame from the zenith pointing series

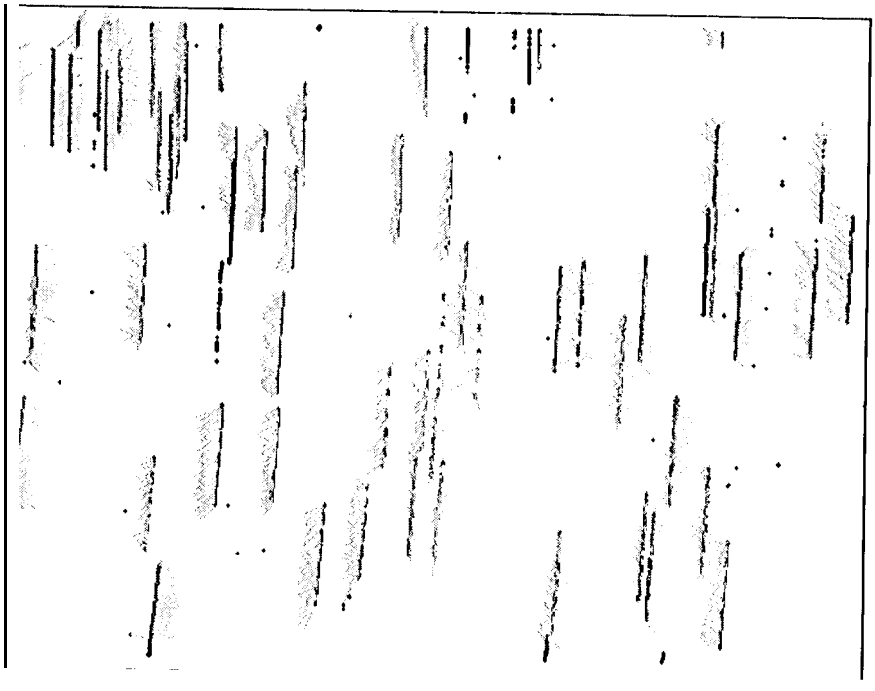

Figure 10. A sequence of error vector diagrams from the zenith pointing series

with result ing improved, overal 1 A SC accuracy.

7. CONCLUSION

'1 'he high level of performance realized by the 1 Danish second generation, star tracker has been veri fied at the premier Northern hemisphere, observing site on Mauna Kea, III. The ASC is different from conventional because it autonomously solves the 10s1 in space problem (initial attitude determination) and determines its attitude relative to celestial coordinates, rather than relative to its CCD image sensor.

The accuracy of tbc ASC has been measured in two ways, the noise equivalent angle (statistical fluctuations) and relative accuracy (including systematic errors). When the low frequencies are removed from the accuracy (due to external terrestrial artifacts), the. relative accuracy is approximately 1.4 arcseconds RMS in pointing and 13 arcseconds RMS in roll. '1 'he systematic. errors have been analyzed with a sequence of error vector diagrams. Potential improvements in accuracy have been identified.

8. ACKNOWLEDGMENT

'1 'he authors would like to thank the ASC Principal Investigator, Professor John 1 .eif Joergensen at the '1'ethnical University of Denmark for his valuable discussions. The work described in this paper was partially carried out by tbc Jet Propulsion Laboratory, California Institute of Technology, under a contract with tbc Nati onal Aeronautics and Space Administration. This work has been sponsored by: Pluto 1 Express, NASA code YSG, the Radioparts Foundation and tbc Technical University of Denmark. Also, thanks to Richard Wainscoat , University of 1 lawaii for facilitating access to tbc observatories of the University of Hawaii on Mauna Kea, Hawaii.

9. REFERENCES

1. The Ørsted Project, Brochure, Computer R esources International, Birkerød, Denmark, 1994.
2. ASTRID 11 reference
3. Hughes 1 Danbury optical systems: 1111-1003 Star tracker, Brochure, 1996, Hughes 1 Danbury Optical ' systems, inc. 100 Wooster J Ieights Road, 1)anbury,(1'1'0681 0-7S89.
4 Ball Aerospace & '1 'echnologies Corp.: CT-602 Star Tracker, Brochure, hall Aerospace Systems Division, P.O. Box 1062, Boulder, Colorado 80306-1062.
5 V.C. Thomas; J.W. Alexander; E. W.Dennison; P.Waddell: Cassini star tracking and identification architecture, S1)l11 Proceedings 2221 p. 15-26.
6. 1{.11. van Bezooijen: '1 'rue sky demonstration of an autonomous star tracker, S1'1 I; Proceedings 2221 p. 156-168.
7. C.C.Liebe: Star trackers for attitude determination, 11 EEE Aerospace and electronics Magazine, June 1995, p. 10-16.
8. Eisenman, A.R.; Joergensen, .1.1,.; Liebe, C.C: Real Sky Performance of tbc Prototype Ørsted Advanced Stellar Compass, 1 EEE Aerospace, Aspen, Co. February 1996, p. x - x.
9. Udomkesmalee S; Alexander, J.W; '1 'olivar, A. F: Stochastic Star Identification, Journal of Guidance, Control, ant] dynamics, Volume 4, number 6, p 1283-1286.
1(). 1,icbc, C.C.: Pattern recognition of Star constellations for Spacecraft applications, 11L111 ; Al ESmagazine, January 93, p.31-39,
11. Shuster, M.D., Oh, S.1).: Three-Axis Attitude determination from vector observations, Journal of Guidance Control and Dynamics, Volume 17, Number 6, p. 1283-12.86.
12.1 Ier majesty's Nautical Almanac office: Royal Greenwich observatory: '1 'he astronomical almanac for the year 1996, 1 IMSO 1995-.
13. Eisenman, A.R.;Liebe, C.C.; Joergensen, 1.1,. :Astronomical